# THERMODYNAMIC ANALYSIS OF A SINGLE EFFECT LITHIUM BROMIDE WATER ABSORPTION SYSTEM USING WASTE HEAT IN SUGAR INDUSTRY

***K. Balaji*** [a*]***, S. Iniyan***[a]***, A. Gurubalan***[b] ***S.R. Senthilkumar***[c]***,***

[a*]*mr.kbalaj@gmail.com,* [b]*gurumariner60@gmail.com,* [c]*srsau@gmail.com*

[a] Dept. of Mechanical Engineering, Anna University, Chennai 600 025, India

[b]Dept. of Mechanical Engineering, IITM, Chennai

[c] Dept. of Mechanical Engineering, Annamalai University, Annamalai nagar 608 002, India

*Energy analysis plays a vital role in the industry due to the use of electrical energy, global warming, and economy crises. This paper describes the waste heat available in the exhaust of the steam turbine and beneficial use of the waste heat. The sugar industry steam turbine exhaust carries enthalpy of steam at 2500 kJ/kg, and this thermal energy can be put into beneficial use as the heat source to the vapor absorption refrigeration system to compensate energy required for DC thyrist motor, and this can also be used for cold storage. Energy savings in terms of cost and fuels are calculated. Investigation on the heat and mass transfer in evaporator has been carried out in vapor absorption system by varying the operating parameter. Less circulation ratio is required to increase the COP. The inlet temperature of the coolant should be less for achieving higher COP.*

**Keywords:** - *Waste heat, lithium bromide water, DC thyrist motor, coefficient of performance*

## Introduction

The sugar industry is one of the leading industries. It produces sugar with the help of sugarcane and also some byproducts like bagasse, molasses, and press mud. These three byproducts are used in different applications where bagasse is used for generating process heat and also for generating the electricity as shown in fig. 1. India is the second largest consumer of sugar, and 19,450 million tons of sugar was produced in 2010 [1]. Rankine cycle is used for generating the electricity, however, the portion of heat energy being wasted even after using a condenser, so this waste heat can be used for pressurizing the vapor absorption machine to cool the DC thyrist room. The increasing $CO_2$ emission and ozone depletion are serious environmental issues due to Chloro Fluoro Carbon present in vapor compression system. These situations evoke new interests in the alternate refrigeration system. The vapor absorption system is near to zero emission technique in which heat energy is available. Economic analysis of vapor absorption system for utilizing waste heat from different heat source was analyzed and reported that absorption heat pump is profitable when it was operating 3000 hours per year [2].

The most usual combinations of working fluids in vapor absorption systems are lithium bromide-water (LiBr-$H_2O$) and ammonia water ($NH_3$-$H_2O$) [3, 4]. Theoretical analysis [5-7] of both systems using waste heat was analyzed. In the LiBr-$H_2O$ system water act as refrigerant whereas, $NH_3$-$H_2O$ system ammonia act as a refrigerant. Ammonia has a high toxic concentration, and also, it

has a major drawback when compared with LiBr-$H_2O$. Crystallization is the recurring problem in LiBr-$H_2O$ system, and it can be overcome by maintaining the temperature. The economic analysis for LiBr-$H_2O$ system using free heat energy was made and concluded that the system is profitable [8]. A conventional absorption system consists of a generator, condenser, evaporator, absorber, solution heat exchanger, solution pump and coolant. The coolant is required to absorb heat from absorber and condenser. The absorbent absorbs evaporated refrigerant on the low-pressure side. Pressurization takes place by the thermal energy supplied at inside the generator.

Theoretical studies of absorption cycle with different working pair reported by the various author. These studies came out with good results [9-10], and also the review highlighted the different work carried out in single effect, multi-effect, half effect absorption systems, sorption and desorption process, GAX cycle, bubble pump [11], diffusion absorption refrigeration, working fluids and small capacity of absorption machine. The author [12] developed the software packages for working pair like $NH_3$-$H_2O$, LiBr-$H_2O$, $ZnBr_2$-Acetone [13], TFE-TEGDME [14, 15] and NH3-$LiNO_3$, and has pointed out the increase in COP with the increase in generator temperature. Compared to other working pair, higher COP achieved while using LiBr-$H_2O$, but it can be operated only in a particular limit because of its crystallization possibility [15]. Effects of auxiliary fluid to enhance the performance in $NH_3$-$H_2O$ was reported [16].

Theoretical and experimental investigation using $ZnBr_2$-Acetone as working pair were done, and the author reported that the system was operating at a generating temperature of 50 ºC without any problem. COP in the range between 0.4 to 0.6 was reported [13, 17]. Some of the new working pairs were studied and reported the performance character [14, 18]. A lot of working pairs were found, but only two ($NH_3$-$H_2O$, LiBr-$H_2O$) were commercialized. Thermodynamic analysis of different parts of the vapor absorption system was analyzed and influences of operating parameters like generator temperature [14, 19], absorber temperature [20], effectiveness of the heat exchanger [21], circulation ratio [14], inlet temperature of water [22] on vapor absorption system using lithium bromide water were reported [23]. The author [23] concluded that generator load decreases with increase in COP, and also increase in temperature of the evaporator reduces the absorber and generator loads.

In this paper, LiBr-$H_2O$ was used as working pair in vapor absorption system. A detailed analysis of available waste heat is presented in our previous work [24]. Specification of DC thyrist room and energy required for cooling the room is given. Design values of each component of the single effect vapor absorption system were given [25]. In this paper, a detailed thermodynamic analysis of the system is given. Also, the effect of cooling water inlet temperature and circulation ratio is analyzed, and most of the authors [26, 27] reported the performance of generator and absorber, but this paper only focuses the evaporator performance and effect of enthalpy of vaporization of the refrigerant in vapor absorption system.

## 2. Energy recovery analysis

### *2.1 Sugar industry data and process*

Fig.1 shows that steam flow from the boiler and the Bagasse was used as a heating source of the boiler for producing steam. The capacity of the boiler was 64 T/h and detail specification of MRK Cooperative Sugar Mill is given in Table. 1. Due to the fluctuation of sugar cane; the total steam flow rate was 36 T/h at the time of analysis. Mass flow rate of the steam was divided into 47% for the high-

pressure steam turbine, and the low-pressure steam turbine was 42.5%, and for the condensing turbine, the steam would be 10.5% at a temperature of 92 ºC to the total capacity. The excavated steam at a temperature of 170 ºC from high-pressure extraction turbine was used for crushing the sugar cane and for pull out juice from sugar cane. The excavated steam at a temperature of 165 ºC from low-pressure extraction turbine was used for heating the juice and producing sugar at various temperatures. There is a huge waste heat available at condensing turbine exhaust. From that, the condensing turbine exhaust is connected with vapor absorption system used for pressurizing the generator. The detail of energy recovery is presented in Table. 2. The cooling water from cooling tower was also used for circulating to the absorber and condenser in the absorption system. The evaporator transferred the heat to the chilled water, and it acts as cold thermal energy storage system. The fan is employed for conditioning the air inside the DC thyrist room.

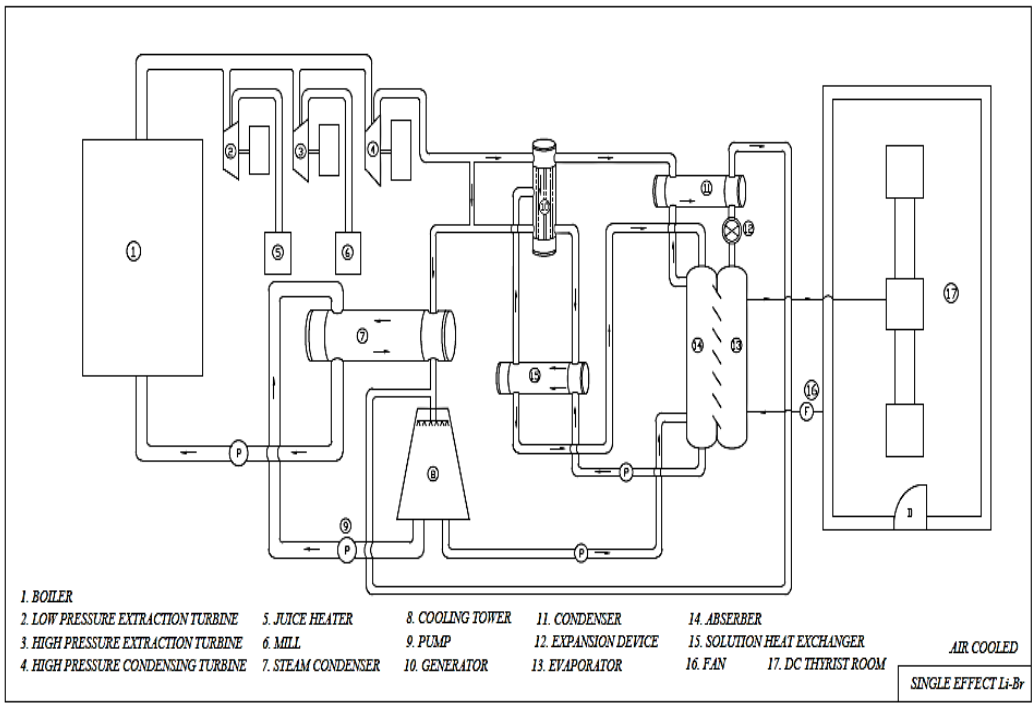


Fig. 1 Layout of vapor absorption refrigeration system using waste heat

**Table: 1 Industry specification**

| Operating parameter | Data |
|---|---|
| Mass flow rate of steam | 3.76 T/h. |
| Temperature of steam | 92 ºC |
| Dryness fraction of steam | 0.93 |
| Efficiency of the boiler | 65% |
| Calorific value of bagasse | 10400 kJ $kg^{-1}$ |
| The selling price of electricity to Tamil Nadu Electricity Board | Rs. 3.25 per kW |
| The plant operated in a year | 210 days |
| Number of vapor compression machine | 4 |
| Capacity of the vapor compression machine | 3TR |
| Vapor compression machine cut off | 2/3 per day |

*2.2 Energy recovery analysis*

**Table: 2 Energy recovery data**

| Energy recovery analysis | Data |
|---|---|
| Annual energy required for cooling DC thyrist motor | 53760 kWh |
| Annual energy required for vapor absorption system (2% VCR) | 1075.2 kWh |
| Annual energy savings | 52684.8 kWh |
| Annual cost saving | Rs. 1, 71,225.6 |
| Total mass of bagasse saved | 87,930.79 kg |
| Total mass of sugar cane saved | 2,93,100 kg |
| Annual cost saving in terms of sugar cane | Rs. 6,44,820 |
| Possibility of operating vapor absorption system from available energy in turbine exhaust | 1995 kW |

## 3. Thermodynamic analysis of vapor absorption system

Temperature analysis and designs are based on the assumption said in the ASHRAE 93. The objective of the design is to increase the coefficient of performance (COP) and heat balance of the absorption heat pump. The system designed for 1995 kW to analyze the requirement of cooling water and mass of steam. First law of thermodynamic was used for the design. Pressure drop and friction loss are neglected. Following factors were assumed for making the design: Inlet temperature of the coolant, evaporation temperature, condensing temperature, mass flow rate of coolant and absorber temperature. Performance analysis was done by varying the evaporator temperature, condenser temperature, and circulation ratio.

*3.1 Working principle of vapor absorption system*

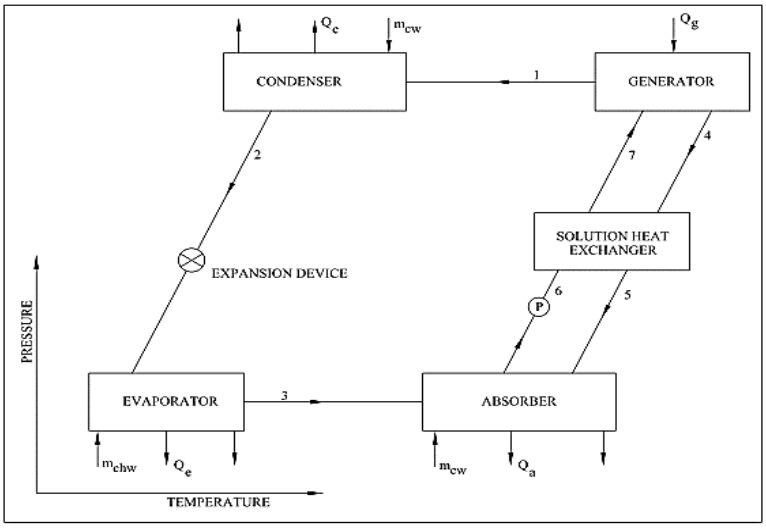


Fig. 2 Pressure and temperature analysis of absorption system

Fig. 2 shows the pressure and temperature different parts of absorption system [28], and it is merged with crystallization chart for avoiding the formation of crystals inside the vapor absorption system. Steam flows into the tube side of the generator, and it rejects the heat to the weak solution. The refrigerant leaves from the weak solution after absorbing the heat, and it became a strong

solution. The refrigerant condensates inside the condenser by removing heat to the water and then moves to the evaporator. The refrigerant evaporated by the chilled water is then absorbed in the absorber, and some of the refrigerant is recirculated. However, the strong solution leaves from the generator, and it rejects the heat in solution heat exchanger. The strong solution absorbs the refrigerant inside the absorber and then circulates to the generator via solution heat exchanger with the help of a pump.

*3.2 Data reduction*

The following assumption was made for the design of absorption refrigeration system [13].

- There is no mass loss in the system
- Friction and pressure drop are neglected
- Condenser pressure is equal to the generator pressure, and the evaporator pressure equal to the absorber pressure
- Only pure refrigerant is evaporated from the generator
- Weak solution leaves the absorber only when it is liquid
- Strong solution leaves the generator at refrigerant temperature
- Refrigerant condensates at condensation temperature

*3.2.1 Generator*

Energy balance in the generator

$$Q_g + (m_{ws} * h_6) - (m_{ss} * h_4) - (m_R * h_1) = 0 \quad (1)$$

Mass balance

$$m_{ws} - m_{ss} - m_R = 0 \quad (2)$$

Equation (1) can be rewritten as

$$Q_g + \left(m_{ws} * C_{p_7} * T_7\right) - \left(m_{ss} * C_{p_4} * T_4\right) - m_R[\left(C_{p_2} * T_2\right) + \left(h_{fg_2}\right) + \left(C_{p_1} * (T_2 - T_1)\right)] = 0 \quad (3)$$

*3.2.2 Condenser*

Energy balance in the condenser

$$Q_c - m_R[\left(h_{fg_2}\right) + \left(C_{p_1} * (T_2 - T_1)\right)] = 0 \quad (4)$$

*3.2.3 Evaporator*

Energy balance in the evaporator

$$Q_e - m_R[\left(h_{fg_3}\right) + \left((C_{p_3} * T_3) - (C_{p_2} * T_2)\right)] = 0 \quad (5)$$

*3.2.4 Solution heat exchanger*

Energy balance in the solution heat exchanger can be written as

$$\left(m_{ws} * C_{p_6} * (T_7 - T_6)\right) - \left(m_{ss} * C_{p_4} * (T_4 - T_5)\right) = 0 \quad (6)$$

$$T_5 = T_1 - \eta_{SHE}\,(T_1 - T_6) = 0 \quad (7)$$

$$T_7 = T_6 + \frac{m_{ss} * C_{p_4}}{m_{ws} * C_{p_6}}\,(T_1 - T_5) = 0 \quad (8)$$

$$\eta_{SHE} = \frac{(T_4 - T_5)}{(T_4 - T_6)} \quad (9)$$

*3.2.5 Absorber*

Energy balance equation can be written as

$$Q_a + \left(m_{ws} * C_{p_6} * T_6\right) - \left(m_{ss} * C_{p_5} * T_5\right) - m_R[\left(C_{p_3} * T_3\right) + \left(h_{fg_3}\right) + \left(C_{p_3} * (T_6 - T_3\right)] = 0 \quad (10)$$

Mass balance can be written as $m_{ws} = m_{ss} + m_R$ (11)

*3.2.6 Coefficient of performance* [29]

The heat required for operating the system is high, compared to the power required for the pump. The pump was too low, so power required for the pump is neglected. COP is defined as the ratio of refrigeration capacity to the generator capacity.

$$COP = \frac{Q_e}{Q_g} \quad (12)$$

*3.2.7 Circulation factor*

It is defined as the ratio of mass flow rate between weak solution and refrigerant, and it is expressed as

$$CR = \frac{m_{ws}}{m_R} \quad (13)$$

*3.2.8 Efficiency ratio*

It is defined as the ratio of coefficient of performance to Carnot coefficient of performance

$$COP_c = (\frac{T_g - T_a}{T_g}) * (\frac{T_e}{T_c - T_e}) \quad (14)$$

$$\eta = \frac{COP}{COP_c} \quad (15)$$

*3.2.9 Overall heat transfer coefficient* [30,31]

The thermal performance of the shell and tube heat exchanger can be written as,

$$Q = U\ A\ LMTD \quad (16)$$

The logarithmic mean temperature difference of the heat exchanger calculated using the following equation:

$$LMTD = \frac{\Delta T_{max} - \Delta T_{min}}{ln\frac{\Delta T_{max}}{\Delta T_{min}}} \quad (17)$$

Overall heat transfer coefficient of shell and tube heat exchanger can be written as,

$$U = \frac{1}{\frac{1}{h_i} + \frac{D_i\, ln(\frac{d_o}{d_i})}{k} + \frac{d_i}{h_o d_o}} \quad (18)$$

*3.2.10 Properties of lithium bromide water solution*

Enthalpy, heat capacity, density, vapor pressure are important properties for the design of vapor absorption system, and the operating limits of 40 to 65% concentration and temperature of 20 to 210 ºC [32]. The author developed a correlation for the above property, and it was adapted for 0 to 75% concentration and temperature range of 0 to 227 ºC [33], properties were given by [34] for the temperature range of 0 to 190 ºC and concentration range of 0 to 75%.

## 4. Result and discussion

*4.1 Effect of cooling water on COP*

The electrical energy consumption in the vapor absorption system was negligible, because compared to supplied thermal energy, it was too low. The energy required for operating the cooling water was lower than air, and the performance of the absorption was based on the inlet temperature of

the coolant. In the case of air as a coolant, the inlet temperature of the coolant will be varied due to the variation in atmospheric temperature, and then it will increase the pressure of the absorber because of the stationary heat of solution inside the absorber, and it will affect the system performance. The constant inlet temperature of the coolant is better even for the low capacity system.

Fig. 3 shows the variation of cooling water inlet temperature on the coefficient of performance. The COP reduces when increasing the weak solution concentration. When increasing the cooling water inlet temperature from 25 ºC to 30 ºC, the COP reduces by 0.05 for 50% weak solution concentration. The variation of COP for the concentration of 54% is 0.13 at an inlet temperature of cooling water from 25 ºC to 30 ºC. The performance improvement at lower weak solution concentration is due to the high mass of absorption rate in the system. The part of cooling water supplied from a cooling tower at a temperature of 27 ºC, and it leaves the condenser at a temperature of 33 ºC. The required mass flow rate of cooling water was too low when compared to condenser from the cooling tower.

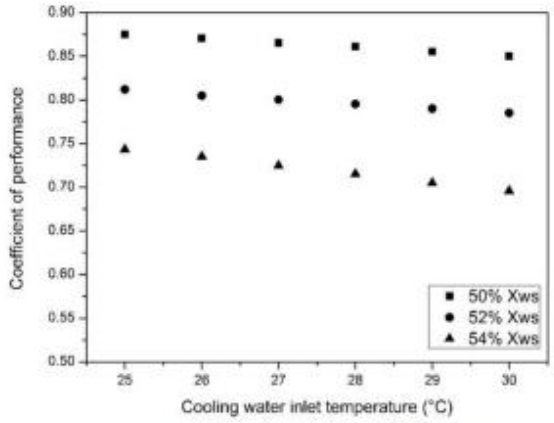


Fig. 3 Impact of cooling water inlet temperature against performance

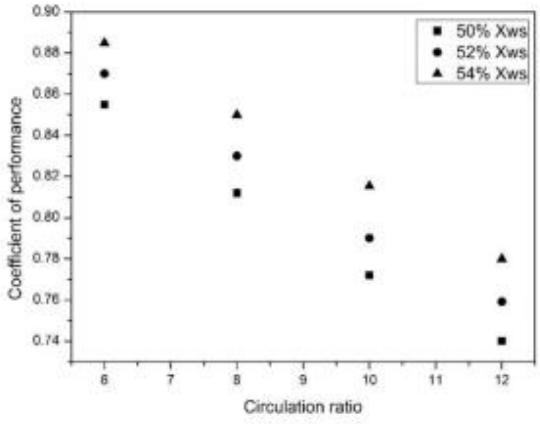


Fig. 4 Impact of circulation ratio on coefficient of performance

*4.2 Effect of circulation ratio on COP*

Circulation ratio is defined as the ratio of the amount of weak solution required for the given refrigeration mass flow rate. Fig. 4 shows the variation of circulation ratio with the coefficient of performance at constant evaporation and condensation temperature. The weak solution concentration varies from 50 to 54%. When the circulation ratio increases the coefficient of performance also decreases. The weak solution remains constant, and it increases the strong solution concentration. When increasing the weak solution concentration, the coefficient of performance also increases, which means it absorbs more refrigerant inside the absorber, and it also increases the mass flow rate of required steam. The generator and absorber load steadily increase when increasing circulation ratio and also increase the flow rate of weak solution. The evaporator load remains constant when increasing the circulation ratio, and it increases the heat of mixing so that coefficient of performance decreases. Whenever the absorber load increases, it reduces the COP because it increases the pressure inside the system, and also, it reduces the absorption coefficient.

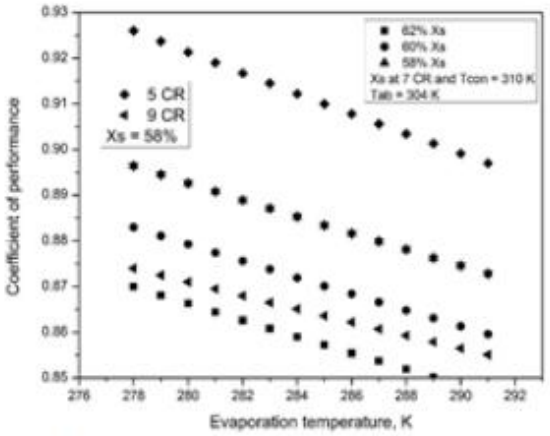


Fig 5 Effect of evaporator temperature on coefficient of performance

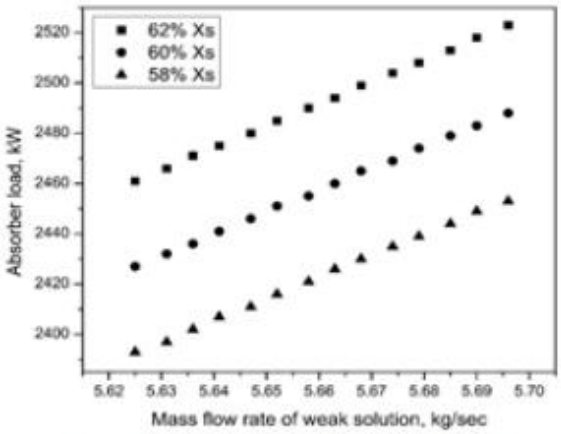


Fig. 6 Variation of absorber load with mass flow rate of weak solution

*4.3 Performance of Evaporator*

Fig. 5 shows the variation in coefficient of performance by changing the evaporator temperature when the condensation and absorption temperatures are 310 K and 304 K respectively. The strong solution concentration and circulation ratio varied from 58 to 62% and 5 to 9 respectively. At constant circulation ratio, the solution, and refrigerant flow rate increases when the evaporator temperature increases. The mass flow rate of required steam was increased by increasing the evaporator load. The coefficient of performance of the vapor absorption was reduced by increasing the evaporator temperature. The strong solution concentration was varied. The lower concentration led to an increase in the coefficient of performance. For the lower circulation ratio, increases the coefficient of performance. Enthalpy of vaporization of the refrigerant is low when increasing the evaporator temperature.

Fig. 6 shows the variation of the absorber load with an increase in the weak solution flow rate when the concentration of the strong solution varied. The absorber load increases when the weak solution flow rate increases at constant strong solution concentration. The concentration of the strong solution increases with increase in absorber load.

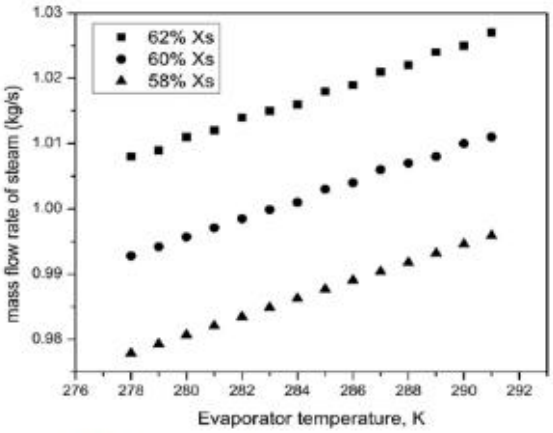


Fig. 7 Effect of evaporator temperature on mass flow rate of hot water

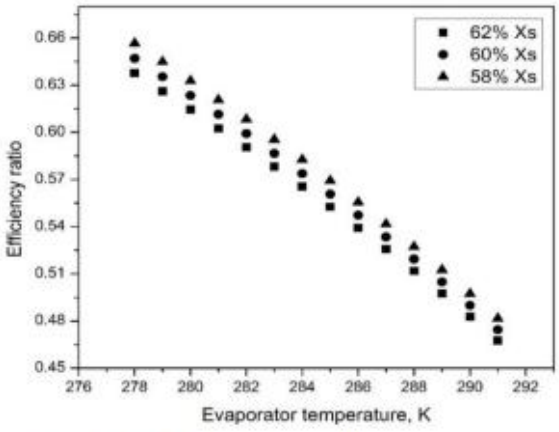


Fig. 8 Effect of evaporator temperature on efficiency ratio

Fig. 7 shows the variation in evaporator temperature with the mass flow rate of steam required at a various concentration of the strong solution. Mass flow rate of steam increases by increasing the evaporator temperature at constant strong solution concentration. The concentration of the strong solution increases with increase in mass flow rate of steam, because of absorber load and enthalpy of refrigerant. Fig. 8 shows the variation of efficiency ratio with evaporator temperature. Efficiency ratio decreases when increasing the evaporator temperature at a particular temperature of the condenser and absorber at constant strong solution concentration. The efficiency ratio is better at a higher condensation temperature and lower evaporation temperature. When strong solution concentration increases, the efficiency ratio decreases. When the evaporator temperature is increased, the generator temperature is reduced and COP. The Carnot COP depends on the temperature of generator and evaporator. Both are indirectly proportional, so it remains constant.

## 5. Conclusion

The mass flow rate of the condensing turbine is 3.76 T/h from which, 1995 kW can be operated with the help of vapor absorption system. If the industry is using the full capacity of the boiler, then the mass flow rate of the condensing turbine will be 6.72 T/h from which 3675 kW can be operated. This cold thermal energy can be used for food storage and human comfort. If the design is made only for the requirement of cooling DC thyrist motor, annual cost saving from the system will be Rs. 1, 71,225.6 and Rs. 6, 44,820 in terms of sugar cane.


## 6. Acknowledgement

This material is based on the work supported by Anna Centenary Research Fellowship (ACRF), Anna University. The primary author express, his sincere thanks to M.R.K. Cooperative sugar mill, Government of Tamil Nadu, Sethiyathope, for providing this opportunity.


## Nomenclature

| | |
|---|---|
| $T$ | Temperature, [K] |
| $N$ | Number of tube |
| $d_i$ | Inner diameter of the tube, [m] |
| $d_0$ | Outer diameter of the tube, [m] |
| $L$ | Length of the tube, [m] |
| $T_s$ | Steam inlet temperature, [$^0$C] |
| $Q$ | Heat load in [kW] |
| $h$ | Enthalpy, [kJkg$^{-1}$] |
| $C_P$ | Specific heat capacity, [kJ kg$^{-1}$ K$^{-1}$] |
| $K$ | Thermal conductivity, [W m$^{-1}$ K$^{-1}$] |
| $A$ | Area, [m$^2$] |
| $V$ | Velocity, [m s$^{-1}$] |
| $Re$ | Reynolds Number, [-] |
| $Nu$ | Nusselt Number, [-] |
| $p_r$ | Prandtl Number, [-] |
| $h_i$ | Average heat transfer coefficient for tube side fluid, [W m$^{-2}$ K$^{-1}$] |
| $h_s$ | Average heat transfer coefficient for shell side fluid, [W m$^{-2}$ K$^{-1}$] |

| | |
|---|---|
| U | Over all heat transfer coefficient, [W $m^{-2}$ $K^{-1}$] |
| LMTD | logarithmic mean temperature difference |
| m | Mass flow rate of solution, [kg $s^{-1}$] |
| X | Concentration, [ %] |
| σ | Surface tension, |
| $COP_c$ | Carnot coefficient of performance |
| η | Efficiency ratio, [-] |
| $\eta_{SHE}$ | Solution heat exchanger efficiency, [%] |
| ρ | Density, [ kg $m^{-3}$] |
| μ | Absolute viscosity, [kg $m^{-1}$ $s^{-1}$] |
| γ | Kinematic viscosity, [ $m^2$ $s^{-1}$] |

**Suffix**

| | |
|---|---|
| ws | weak solution |
| ss | strong solution |
| R | Refrigerant |
| W | Wall |
| a | absorber |
| c | Condenser |
| g | Generator |
| e | Evaporator |
| SHE | Solution heat exchanger |
| l | liquid |
| v | vapor |
| 1,2,3,4,5,6 | Various points as shown in fig.2 |

**7. References**

[1] M.K. Chauhan, Varun, S. Chaudhary, S. Kumar, Samar, Life cycle assessment of sugar industry: A review, Renewable and Sustainable Energy Reviews, 15 (2011) 3445-3453.

[2] S. Brückner, S. Liu, L. Miró, M. Radspieler, L.F. Cabeza, E. Lävemann, Industrial waste heat recovery technologies: An economic analysis of heat transformation technologies, Applied Energy, 151 (2015) 157-167.

[3] M.U. Siddiqui, S.A.M. Said, A review of solar powered absorption systems, Renewable and Sustainable Energy Reviews, 42 (2015) 93-115.

[4] L.F. Mendes, M. Collares-Pereira, F. Ziegler, A rich solution spray as a refining method in a small capacity, single effect, solar assisted absorption machine with the pair NH3/H2O: Experimental results, Energy Conversion and Management, 48 (2007) 2996-3000.

[5] K. Ebrahimi, G.F. Jones, A.S. Fleischer, Thermo-economic analysis of steady state waste heat recovery in data centers using absorption refrigeration, Applied Energy, 139 (2015) 384-397.

[6] A. Ramanathan, P. Gunasekaran, Simulation of absorption refrigeration system for automobile application, Thermal science, 12 (2008),3, 5-13.

[7] A. Sathyabhama, T. Ashok Babu, Thermodynamic simulation of ammonia-water absorption refrigeration system, Thermal science, 12 (2008), 3, 45-53.

[8] A. Buonomano, F. Calise, M. Vicidomini, A dynamic model of an innovative high-temperature solar heating and cooling system. Thermal science, 20 (2016) 1121-1133.
[9] P. Srikhirin, S. Aphornratana, S. Chungpaibulpatana, A review of absorption refrigeration technologies, Renewable and Sustainable Energy Reviews, 5 (2001) 343-372.
[10] J.M. Labus, J.C. Bruno, A. Coronas, Review on absorption technology with emphasis on small capacity absorption machines, Thermal science, 17 (2013) 739-762.
[11] Benhmidene, B. Chaouachi, M. Bourouis, S. Gabsi, Effect of operating conditions on the performance of the bubble pump of absorption-diffusion refrigeration cycles, Thermal science, 15 (2011), 3, 793-806.
[12] M.I. Karamangil, S. Coskun, O. Kaynakli, N. Yamankaradeniz, A simulation study of performance evaluation of single-stage absorption refrigeration system using conventional working fluids and alternatives, Renewable and Sustainable Energy Reviews, 14 (2010) 1969-1978.
[13] S. Ajib, A. Karno, Thermo physical properties of acetone–zinc bromide for using in a low temperature driven absorption refrigeration machine, Heat and Mass Transfer, 45 (2008) 61-70.
[14] A. Coronas, M. Vallés, S.K. Chaudhari, K.R. Patil, Absorption heat pump with the TFE-TEGDME and TFE-H2O-TEGDME systems, Applied Thermal Engineering, 16 (1996) 335-345.
[15] A. Genssle, K. Stephan, Analysis of the process characteristics of an absorption heat transformer with compact heat exchangers and the mixture TFE–E181, International Journal of Thermal Sciences, 39 (2000) 30-38.
[15] M. Izquierdo, M. Venegas, P. Rodríguez, A. Lecuona, Crystallization as a limit to develop solar air-cooled LiBr–H2O absorption systems using low-grade heat, Solar Energy Materials and Solar Cells, 81 (2004) 205-216.
[16] A. Coronas, Refrigeration absorption cycles using an auxiliary fluid, Applied Energy, 51 (1995) 69-85.
[17] A. Karno, S. Ajib, Thermodynamic analysis of an absorption refrigeration machine with new working fluid for solar applications, Heat and Mass Transfer, 45 (2008) 71-81.
[18] S. Jian, F. Lin, Z. Shigang, Performance calculation of single effect absorption heat pump using LiBr + LiNO3 + H2O as working fluid, Applied Thermal Engineering, 30 (2010) 2680-2684.
[19] M. Kilic, O. Kaynakli, Second law-based thermodynamic analysis of water-lithium bromide absorption refrigeration system, Energy, 32 (2007) 1505-1512.
[20] S.C. Kaushik, A. Arora, Energy and exergy analysis of single effect and series flow double effect water–lithium bromide absorption refrigeration systems, International Journal of Refrigeration, 32 (2009) 1247-1258.
[21] C. Ezgi, Design and thermodynamic analysis of an H2O–LiBr AHP system for naval surface ship application, International Journal of Refrigeration, 48 (2014) 153-165.
[22] O. Kaynakli, The first and second law analysis of a lithium bromide/water coil absorber, Energy, 33 (2008) 804-816.
[23] O. Kaynakli, M. Kilic, Theoretical study on the effect of operating conditions on performance of absorption refrigeration system, Energy Conversion and Management, 48 (2007) 599-607.
[24] K. Balaji, R. Ramkumar, Study of Waste Heat Recovery From Steam Turbine Xhaust for Vapor Absorption System in Sugar Industry, Procedia Engineering, 38 (2012) 1352-1356.
[25] K. Balaji, R.S. Kumar, Study of Vapor Absorption System Using Waste Heat in Sugar Industry, IOSR Journal of Engineering, 2 (2012) 34-39

[26] M. Vallès, M. Bourouis, D. Boer, A. Coronas, Absorption of organic fluid mixtures in plate heat exchangers, International Journal of Thermal Sciences, 42 (2003) 85-94.
[27] M. Medrano, M. Bourouis, A. Coronas, Double-lift absorption refrigeration cycles driven by low–temperature heat sources using organic fluid mixtures as working pairs, Applied Energy, 68 (2001) 173-185.
[28] B.H. Gebreslassie, M. Medrano, D. Boer, Exergy analysis of multi-effect water–LiBr absorption systems: From half to triple effect, Renewable Energy, 35 (2010) 1773-1782.
[29] T.K. Gogoi, K. Talukdar, Exergy based parametric analysis of a combined reheat regenerative thermal power plant and water–LiBr vapor absorption refrigeration system, Energy Conversion and Management, 83 (2014) 119-132.
[30] O. Kaynakli, Exergy analysis of absorber using water/lithium bromide solution, Heat and Mass Transfer, 44 (2007) 1089-1097.
[31] A. Karno, S. Ajib, Effect of tube pitch on heat transfer in shell-and-tube heat exchangers—new simulation software, Heat and Mass Transfer, 42 (2005) 263-270.
[32] Y. Kaita, Thermodynamic properties of lithium bromide–water solutions at high temperatures, International Journal of Refrigeration, 24 (2001) 374-390.
[33] J. Pátek, J. Klomfar, A computationally effective formulation of the thermodynamic properties of LiBr–H2O solutions from 273 to 500 K over full composition range, International Journal of Refrigeration, 29 (2006) 566-578.
[34] H.T. Chua, H.K. Toh, A. Malek, K.C. Ng, K. Srinivasan, Improved thermodynamic property fields of LiBr–H2O solution, International Journal of Refrigeration, 23 (2000) 412-429.